Hindawi
Journal of Food Biochemistry
Volume 2024, Article ID 9971510, 15 pages
https://doi.org/10.1155/2024/9971510

Research Article

Salidroside Alleviates Myocardial Ischemia Reperfusion by Balancing Mitochondrial Homeostasis via Nrf2

Tingxu Yan,[1,2] **Xu Li**,[1] **Xin Wang**,[1] **Bosai He**,[2] **Ying Jia**,[2] **and Wei Xiao**[1]

[1]*Jiangsu Kanion Pharmaceutical Co., Ltd., Lianyungang 222047, China*
[2]*School of Functional Food and Wine, Shenyang Pharmaceutical University, Wenhua Road 103, Shenyang 110016, China*

Correspondence should be addressed to Ying Jia; jysyphu@163.com and Wei Xiao; xw_kanion@163.com

Received 13 December 2023; Revised 6 February 2024; Accepted 7 February 2024; Published 14 February 2024

Academic Editor: Rong He

Salidroside (SAL), a phenylpropanoid glycoside compound mainly from Rhodiola rosea, showed potential effects on myocardial ischemia reperfusion (MIRI) in our previous studies. The primary objective of this investigation was to study the mechanism by which SAL preserves mitochondrial homeostasis in order to provide protection against MIRI. The impact of SAL on the hypoxia/reoxygenation (H/R)-induced H9c2 cells was detected by using CCK-8, LDH, and AST. The number, function, and morphology of mitochondria were examined by TEM, RT-qPCR, and western blot. The binding ability between SAL and Nrf2 was explored through molecular docking and the cell thermal shift assay. Combined with the Nrf2 inhibitor ML385, our results demonstrated that SAL promotes mitochondrial protection by activating Nrf2, decreasing oxidative stress, and altering the AMPK/PGC-1α/PPARα pathway. In addition, SAL elevates ATP levels and improves mitochondrial dynamics imbalance by inducing both autophagy and mitophagy. These findings highlight the potential therapeutic benefits of SAL for cardiac health and the mitigation of MIRI.

1. Introduction

Myocardial hypoxia and energy failure of cardiomyocytes lead to the development of acute myocardial infarction (AMI), which is characterized by myocardial necrosis [1]. The most effective treatments for this disease include reperfusion therapy, cardiopulmonary resuscitation, cardiac transplantation, and recanalization of the shocked organ. However, these therapies can lead to more significant harm to cardiomyocytes and induce apoptosis, thereby disrupting the heart's structure and function. This phenomenon is commonly mentioned as myocardial ischemia-reperfusion injury (MIRI) [2]. Therefore, exploring the pathogenesis of MIRI and finding effective prevention and treatment drugs are becoming a hot spot in clinical research.

MIRI is regulated by a variety of complex mechanisms, and numerous studies have indicated that the pathogenesis of cardiovascular diseases is closely linked to the substantial impairment of mitochondria, so maintaining the healthy state of mitochondria in cardiomyocytes can help maintain cardioprotection [3, 4]. Nrf2, a nuclear factor related to erythroid-2, serves as a transcription factor essential for sustaining proper mitochondrial function and protecting the cellular defense system from oxidative stress [5]. In the realm of MIRI, the impairment of mitochondria results in an imbalance of mitochondrial dynamics, with escalated mitochondrial fission [6] and reduced mitochondrial fusion [7]. Consequently, there is a significant accumulation of fragmented mitochondria, disrupting the homeostasis of the mitochondrial genome [8], which makes myocardial cell damage more severe [9]. Prior research has documented an association between decreased Nrf2 levels and the imbalanced abundance of proteins involved in mitochondrial dynamics, including Drp1, OPA1, and Mfn1/2. Consequently, this imbalance contributes to the disruption and impairment of mitochondrial function [10, 11]. The enhancement of the AMPK/Nrf2 pathway has the potential to enhance mitochondrial fission, thereby facilitating energy provision and cell viability [12, 13], and heightened Nrf2 functionality leads to an increase in the proteasome's

activity, thereby facilitating the degradation of Drp1, a protein crucial for mitochondrial fission [14]. Furthermore, research findings have indicated that oxidative stress during MIRI triggers apoptosis in cardiomyocytes, whereas autophagy is suppressed [15]. Therefore, activation of autophagy in the stage of MIRI and removal of damaged cells and organelles can well achieve the protective effect of cardiomyocytes [16]. The regulation of autophagy, particularly mitophagy, is influenced by Nrf2, as demonstrated in previous studies [17, 18]. In the absence of Nrf2, autophagic turnover decreases, leading to substantial buildup of p62 and a reduction in LC3-II levels. These findings indicate that the activation of Nrf2 is crucial for the dependence of autophagy [19–21]. Mitophagy is a form of autophagy, which mainly regulates the quality and quantity of mitochondria by removing and degrading aging and damaged mitochondria, thereby maintaining the dynamic balance between mitochondria and cells [22]. Without the presence of Nrf2, Keap1 initiates the degradation process of Miro2. Miro2 is a protein found in the outer membrane of mitochondria. It plays a crucial role as a receptor for Parkin, which is responsible for selectively removing damaged mitochondria through a process known as mitophagy [23]. Hence, the strategy of targeting Nrf2 and regulating mitochondrial homeostasis may potentially prove effective in alleviating MIRI.

SAL is one of the main bioactive components of Rhodiola Rosea. Pharmacological studies have shown that SAL has antifatigue, hypoxia resistance, antiaging, protein metabolism, anti-inflammatory, cardiotonic, and antitumor effects [24]. Its nontoxic and nonaddictive properties have gained national recognition as a source of healthcare medicine and food. Our previous studies found that SAL could attenuate apoptosis in H/R-exposed H9c2 cells and ischemia/reperfusion-injured rats by the IGF1R/PI3K/AKT signaling pathway [25]. Moreover, SAL successfully reinstated the potential of the mitochondrial membrane both *in vitro* and *in vivo*, which suggested that mitochondria might participate in the cardioprotective benefits of SAL. Henceforth, the present study aims to clarify the mechanism by which SAL maintains equilibrium in mitochondrial homeostasis for mitigating MIRI, focusing on the modulation of Nrf2.

2. Materials and Methods

2.1. Materials. SAL (purity >98%) and trimetazidine (purity >98%) were acquired from MeilunBio (Dalian, China), and both drugs were dissolved in dimethyl sulfoxide (DMSO, Solarbio Science & Technology Co.). They were stored at a temperature of −20°C until they needed to be utilized. To prevent cytotoxicity, the concentration of DMSO in the subsequent experiments was reduced to less than 1% by diluting it with the DMEM complete medium.

2.2. Cell Culture and Treatment. The H9c2 cardiac myoblast cell line derived from the rat myocardium (Cell Line Bank of Shanghai BioScience Co., Ltd., China) was cultivated in DMEM (Dalian Meilun Biotechnology Co., Ltd., China), containing 110 mg/L of high glucose, L-glutamine, and sodium pyruvate. In addition, the medium was supplemented with 10% (v/v) FBS (ScienCell Research Laboratories, US) and 1% penicillin-streptomycin (Meilun Biotech, China). The cells were cultured in a controlled environment with a temperature of 37°C and an air mixture of 95% air and 5% CO_2.

Upon achieving 80–90% confluence, the H/R model protocol was followed. SAL and trimetazidine were dissolved in the cell culture media, and subsequently, the H9c2 cells were pretreated with SAL (50 and 100 μM) or trimetazidine (at a concentration of 50 μM) for a duration of 12 hours, which regard trimetazidine as a masculine drug. To induce hypoxia, cells in all groups were incubated in a hypoxia incubator chamber at 37°C for 4 hours, except for the control group. In this process, DMEM was substituted with glucose-free and FBS-free Hank's Balanced Salt Solution (provided by Meilun Biotech, China). The hypoxia incubator chamber contained 5% (v/v) CO_2 and 1% O_2, 94% (v/v) N_2. To enable reoxygenation, the cells were cultured for 3 hours using DMEM (10% FBS) instead of HBSS at 37°C and 5% CO_2. During hypoxia and reoxygenation, SAL and trimetazidine were all dissolved in DMEM and Hank's Balanced Salt Solution.

2.3. Cell Viability Analysis. We evaluated the viability of H9c2 cells via the CCK-8 assay following SAL treatment. The H9c2 cell culture was initiated by seeding 1×10^4 cells per well in 96-well plates. Following various experimental interventions, a 10 μL solution of CCK-8 was introduced into per well and incubated for a duration of 2 hours at 37°C in a CO_2 incubator with a 5% CO_2 atmosphere. The assessment of cell viability was performed by employing a microplate reader to measure the optical density at a wavelength of 450 nm (Thermo Scientific, China).

2.4. Lactate Dehydrogenase Release Assay. To evaluate LDH viability following different treatments, we employed the lactate dehydrogenase (LDH) leakage assay (Nanjing Jiancheng Bioengineering Institute, China). A microplate reader was utilized to detect optical density at 450 nm, allowing the determination of LDH concentration. The obtained results were subsequently expressed as U/L.

2.5. ATP Detection. We quantified cellular adenosine triphosphate (ATP) levels by employing a fluorescence technique with the ATP assay kit (Beyotime, China), as described in previous studies (Genmed Scientifics Inc.). As per the guidelines provided by the manufacturer, the multimode plate reader (PerkinElmer Management Co., ltd.) was employed to measure the RLU. To determine the ATP concentration in the samples, the RLU of the samples is compared to the standard curve.

2.6. Enzyme-Linked Immunosorbent Assay (ELISA). The amounts of GSH, MDA, CTn-T, and SOD were assessed using the kit assay. The manufacturer's protocols were

followed, and the measurements were taken spectrophotometrically at a wavelength of 450 nm. To determine the concentrations of CTn-T, SOD, MDA, and GSH, the O.D. of the samples was compared to the standard curve.

2.7. Detection of ROS. The ROS assay kit (Meilun Biotech, China) was utilized to determine the ROS level, which involves a fluorescent dye that is based on the change in the fluorescence intensity of DCFH-DA (2,7-dichlorodihydrofluorescein diacetate). In order to accomplish this, H9c2 cells were seeded in a 6-well plate with a density of 2.5×10^5 cells per well and subsequently treated with the appropriate concentrations of SAL. Subsequent to PBS washing, the cells were incubated with 5 μM DHE at 37°C for 30 minutes, following the manufacturer's instructions. Flow cytometry (Accuri C6, BD) was performed to measure ethidium fluorescence (emission at 529 nm nm, excitation at 495) immediately. The FlowJo V10 software was employed to calculate the levels of superoxide anions.

2.8. Transmission Electron Microscopy (TEM). To conduct a comprehensive investigation into the structure of mitochondria, transmission electron microscopy (TEM) was employed. The technique described earlier was employed to obtain tomograms from sections using a TECNAI G2 SPIRIT transmission electron microscope (PEI).

2.9. Molecular Docking Studies. To explore the potential binding mode between compound SAL and protein Nrf2, AutoDock software was utilized for conducting molecular docking analysis. The PDB format of the 3D structure of SAL was acquired from the Pubchem database (https://pubchem.ncbi.nlm.nih.gov/) and then changed to mol2 format using Open Babel 3.1.1 software. Prior to docking, the AutoDockTools 1.5.7 software optimized the structure. In addition, the crystal structure of Nrf2 complexed with its classic resveratrol (PDB ID = 5CGJ) was acquired from the RCSB Protein Data Bank (http://www.pdb.org) and optimized before docking using AutodockTools 1.5.7, saved as pdbqt format. AutoDockTools was utilized for creating docking input files, and the Vina docking score was utilized to select the best-scoring pose, which was subsequently visually analyzed using PyMoL 1.7.6 software.

2.10. Cellular Thermal Shift Assay (CETSA). The CETSA experiment followed the methods outlined in previous studies. To initiate the experiment, cells were first seeded and then treated either with 50 μM SAL or 1% DMSO for a duration of 12 hours at a temperature of 37°C. Afterwards, the cells were collected and individually heated at various temperatures (45°C, 48°C, 51°C, 53°C, 56°C, 59°C, 61°C, 63°C, and 69°C). Each heating duration was set to 10 minutes. Then, the resulting samples were subjected to centrifugation, and the cells obtained from this process were analyzed using western blotting techniques.

2.11. Isolation of Mitochondria. Mitochondrial isolation was carried out by employing Cell Mitochondria Isolation Kit as per the manufacturer's protocol. Briefly, cells were washed two times with PBS, harvested, and then centrifuged. A glass homogenizer (Solarbio, YA0853) was used to transfer and homogenize the resulting cell pellets. The homogenization process was repeated 10–30 times in total. Subsequently, after centrifuging the homogenate at 600 g for 10 minutes at 4°C, the clear liquid portion above the sediment was carefully removed, and the compacted residue, which contains mitochondria, was retained for further experimentation.

2.12. RNA Isolation and RT-qPCR. The Nanodrop One/Onec spectrophotometer (Thermo Fisher, China) was employed to assess the concentration and purity of RNA samples obtained from H9c2 cells using TRIzol® reagent, following the instruction provided by the manufacturer. According to the protocol provided by the manufacturer, the PrimeScript RT reagent kit was utilized to perform reverse transcription of total RNA into cDNA [26]. The internal reference gene chosen for this study was GAPDH. The quantification of mRNA levels of the target gene involved the utilization of the 2-ΔΔcq approach. Primer sequences used for RT-qPCR are shown in Table 1.

2.13. Western Blotting Assay. Following SAL treatment, the H9c2 cells were gathered and lysed through the addition of a specific amount of lysis solution comprising PMSF. The resulting mixture was then subjected to centrifugation at 4°C to isolate the supernatant, which was subsequently utilized to determine the protein concentration utilizing the BCA kit. Subsequent to electrophoresis, the gels were moved onto preactivated NC membranes. To block any nonspecific binding, the membranes were incubated in a solution containing 5% fat-free milk in TBST buffer for a duration of 90 minutes. Following this blocking step, the membranes were subjected to primary antibodies at a temperature of 4°C for the duration of the night. Following overnight incubation, the primary antibodies were collected and subjected to three successive washes using TBST for 15 minutes each. The primary antibodies for the western blotting assay were as follows: Nrf2 (1 : 1000, Proteintech, #16396), SIRT1 (1 : 1000, Abcam, #ab110304), Beclin1 (1 : 1000, CST, #3495), AMPK (1 : 1000, Abcam, #ab131512), HO-1 (1 : 1000, Proteintech, #10701), PGC-1α (1 : 1000, Abcam, #ab176328), PPARα (1 : 1000, CST, #74076), COX IV (1 : 1000, CST, #4850), TOMM20 (1 : 1000, Abcam, #ab186735), VDAC1 (1 : 1000, Abcam, #ab154856), LAMP2 (1 : 1000, Proteintech, #27823), ATG5 (1 : 1000, Proteintech, #10181), LC3B (1 : 1000, Proteintech, #18725), Parkin (1 : 1000, CST, #32833), PINK1 (1 : 1000, Proteintech, #23274), and β-actin (1 : 1000, Proteintech, #8115). The secondary antibody incubation on the membrane lasted for 1.5 hours at room temperature, followed by 3 washes with TBST for 15 minutes each. The membrane was finally placed on the ChemiDoc™ instrument (BIO-RAD, CA, USA), an appropriate amount of luminescent solution was added dropwise to take pictures, and the

Table 1: Primer sequences used for RT-qPCR.

Primers	Primer sequences (5′-3′)
OPA1	Forward: ATCATCTGCCACGGGTTGTT Reverse: GAGAGCGCGTCATCATCTCA
Mfn1	Forward: ATGAGATTTGTCGCCTGTC Reverse: ATGCCATCTTCTATGTGCTT
Mfn2	Forward: GAGTGTCAAGACGTGAACCA Reverse: CATCCAGGCAAAACTTATCAATCCA
Fis1	Forward: GCACGCAGTTTGAATACGCC Reverse: CTGCTCCTCTTTGCTACCTTTGG
DRP1	Forward: CATGGCTTTGGATGGAGAGT Reverse: TGGGAGTTTGCTCTTCAAGG
GAPDH	Forward: GGCACAGTCAAGGCTGAGAATG Reverse: ATGGTGGTGAAGACGCCAGTA

images were analyzed in the grey scale using the Image-Pro Plus 6.0 software.

2.14. Immunofluorescence Staining. The cell slides were placed in 24-well plates, following a 24-hour culture period. To initiate fixation of the H9c2 cells, methanol was applied at a low temperature for 20 minutes. Subsequently, 1 mL of PBS was applied for cleansing, followed by the addition of 0.5% Triton X-100 for penetration. Once the cleansing process was completed, sealing was carried out using a 5% BSA solution at room temperature for 1.5 hours. JC-1 primary antibodies, which had been prepared in advance, were then added and incubated at 4°C for 12 hours. Following a cleaning step with PBST, the preconfigured fluorescent secondary antibody was introduced and incubated for one hour at room temperature, while keeping the environment dark. Finally, the samples were carefully observed and photographed using an inverted fluorescence microscope.

2.15. Statistical Analysis. The results are expressed as mean ± SD. Differences between the groups were analyzed by one-way ANOVA with Tukey's multiple comparisons test by GraphPad Prism (San Diego, CA, USA). Statistical significance was determined at a P value of less than 0.05, indicating significant differences among the groups.

3. Results

3.1. SAL Ameliorated H/R-Induced Injury in H9c2 Cells. Cell viability assessments were utilized to evaluate the impact of SAL on cell viability in H/R-exposed H9c2 cells. Our findings revealed that SAL, even at concentrations as high as 1600 μM, did not show any noteworthy cytotoxicity (Figure 1(a)). After the occurrence of H/R injury, there was a noticeable decrease in the proliferation of the H9c2 cells. Pretreatment with SAL resulted in a significant increase in cell proliferation subsequent to H/R injury (Figure 1(b)). As for alterations of the myocardial zymogram, a substantial increase in the levels of CTn-t, AST, and LDH was detected in H/R-induced H9c2 cells. 50 μM SAL and 100 μM SAL groups significantly reduced these activities, respectively (Figures 1(c)–1(e)). These results demonstrate the cardioprotective properties of SAL in cell injury induced by H/R.

3.2. SAL Alleviated H/R-Induced Oxidative Stress in H9c2 Cells. The flow cytometry analysis exhibited that SAL treatment could mitigate the excessive generation of ROS induced by H/R (Figure 2(a)), Furthermore, the amounts of SOD, GSH, and MDA, which are known to possess antioxidant properties, displayed a significant decrease in the cardiomyocytes treated with HR (Figures 2(b)–2(d)). Subsequently, to delve into the mechanistic aspects of SAL, we proceeded to examine its impact on the expression of HO-1 and Nrf2 proteins in H9c2 cells subjected to H/R-induced injury. The findings from the western blotting assay revealed that Nrf2 and HO-1 expressions were reduced following H/R injury (Figures 2(e)–2(g)). Intriguingly, the expressions of HO-1 and Nrf2 were reversed upon SAL treatment. Consequently, these results substantiate the significance of SAL in mitigating oxidative stress in cardiomyocytes.

3.3. SAL Attenuated H/R-Induced Mitochondrial Dysfunction in H9c2 Cells. The survival and function of cardiomyocytes heavily rely on the essential role played by mitochondrial function. In this study, we explored the quantification of the number of mitochondria using TEM. The findings exhibited a remarkable reduction in the quantity of mitochondria within H/R-triggered H9c2 cells in contrast to the control cohort, which witnessed a significant enhancement through the implementation of SAL intervention (Figure 3(a)). PGC-1α plays a crucial role in regulating mitochondrial proliferation, while AMPK, SIRT1, PGC-1α, and PPARα are all involved in governing both mitochondrial biogenesis and mitochondrial homeostasis. According to the western blotting analysis illustrated in Figures 3(b)–3(f), it was observed that HR injury led to the suppression of AMPK, SIRT1, PGC-1α, and PPARα. Notably, the administration of SAL exhibited the ability to enhance the expression levels of AMPK, PGC-1α, and PPARα within H9c2 cells. However, SAL did not show any noteworthy impact on SIRT1 protein expression. In general, the findings presented demonstrated that SAL-induced activation of AMPK/PGC-1α/PPARα has a positive impact on enhancing mitochondrial function and bolstering mitochondrial energy metabolism in H/R-injured H9c2 cells. HR treatment led to a decrease in overall ATP synthesis in the H9c2 cells, suggesting that ATP production was suppressed by HR (Figure 3(g)). However, 50 μM and 100 μM SAL treatments improved ATP generation, and the same results were observed in JC-1 staining as well (Figure 3(h)). The above results demonstrate that SAL can improve H/R-induced mitochondrial dysfunction.

3.4. SAL Improved Mitochondrial Dynamics in the H/R-Induced H9c2 Cells. The recent focus on mitochondrial fusion/fission dynamics has highlighted its significant contribution to maintaining mitochondrial homeostasis. First, we investigated mitochondrial morphology using

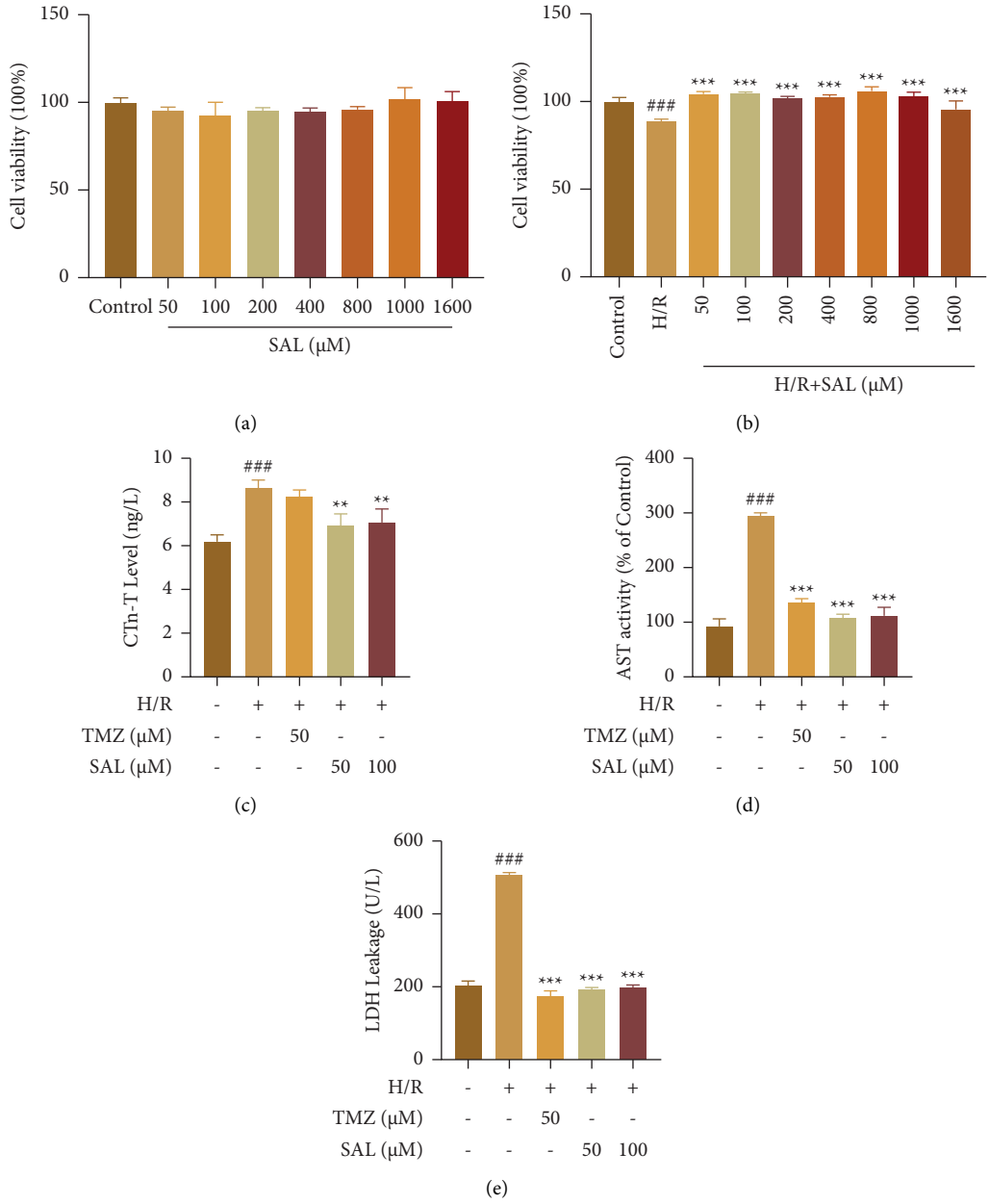

Figure 1: Myocardial protection by SAL against H/R. (a, b) Cell viability of H9c2 cells treated with SAL (0–1600 μM). (c–e) The AST, CTn-T, and LDH release of H9c2 cells treated with SAL (50–100 μM) followed by H/R stimulation. Values are presented as mean ± SEM. $^{\#\#\#}P < 0.001$ versus the control group; $^{**}P < 0.01$ and $^{***}P < 0.001$ versus the H/R group.

TEM. In contrast to the control group, the cristae of the mitochondria in the H/R group were broken and the mitochondria were vacuolated, indicating severe mitochondrial damage, whereas the administration of SAL treatment induced notable alterations in mitochondrial morphology and a tight mitochondrial structure (Figure 4(a)). In the H9c2 cells treated with H/R, a significant decrease in the expression of VDAC1, COX IV, and TOMM20 (proteins marking the mitochondria) was observed compared to that in the control group. Notably, the expression of these aforementioned proteins was enhanced upon SAL administration (Figure 4(b)). qRT-PCR *in vitro* demonstrated that Mfn1, Mfn2, and OPA1 (mitochondrial fusion-related proteins) were repressed by HR injury, and DRP1 and Fis1 (mitochondrial fission-related proteins) were activated by H/R injury. It is worth mentioning that SAL treatment reversed the levels of both fusion-related and fission-related proteins involved in mitochondrial dynamics (Figure 4(c)).

3.5. SAL Improved Autophagy and Mitophagy in the H/R-Induced H9c2 Cells. To further investigate the mechanism of myocardial protection exerted by SAL, we examined the changes in autophagy-related indicators. First, we investigated the autophagosome using TEM. In the H/R group, a noticeable reduction occurred in the count of autophagic

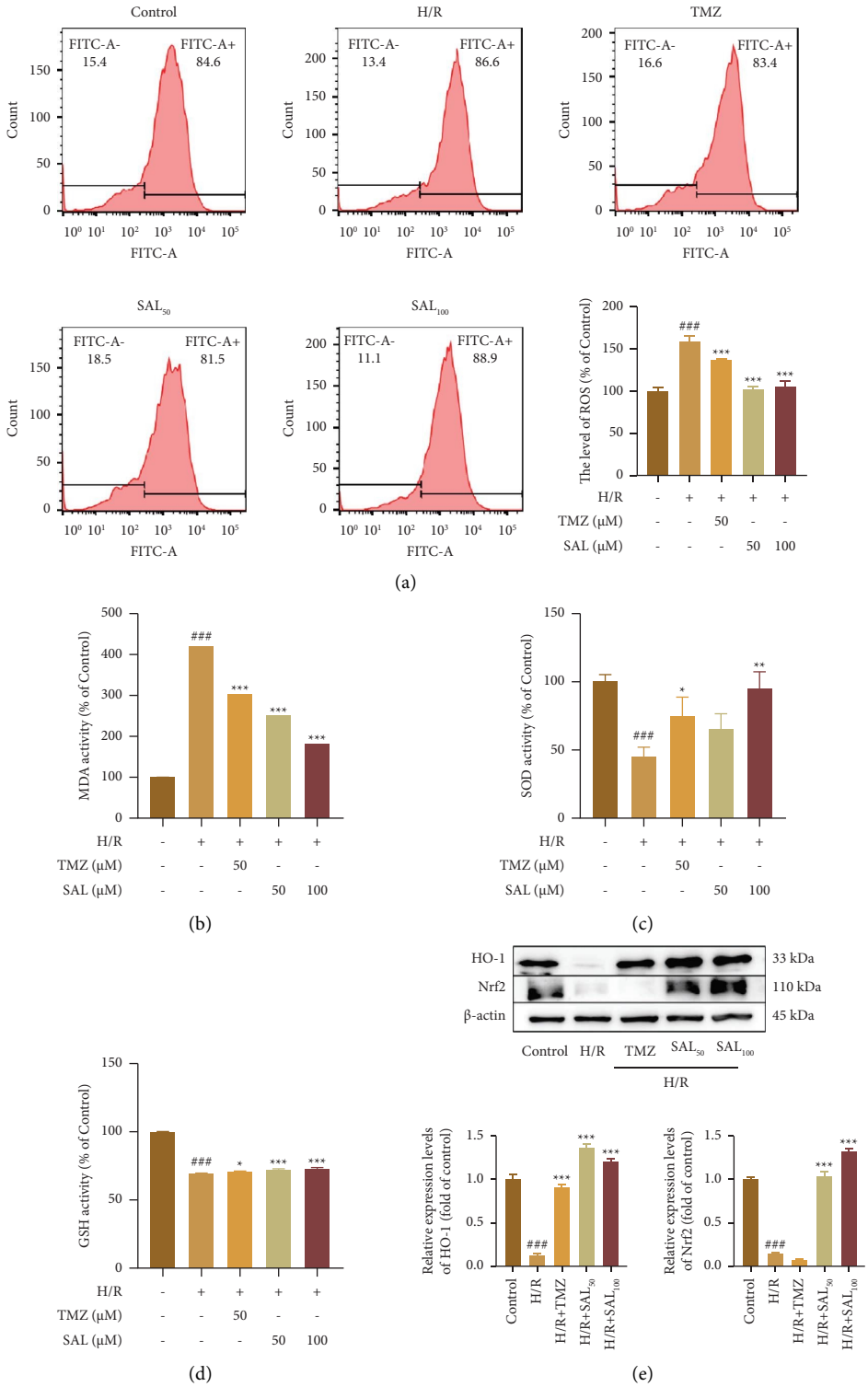

Figure 2: Continued.

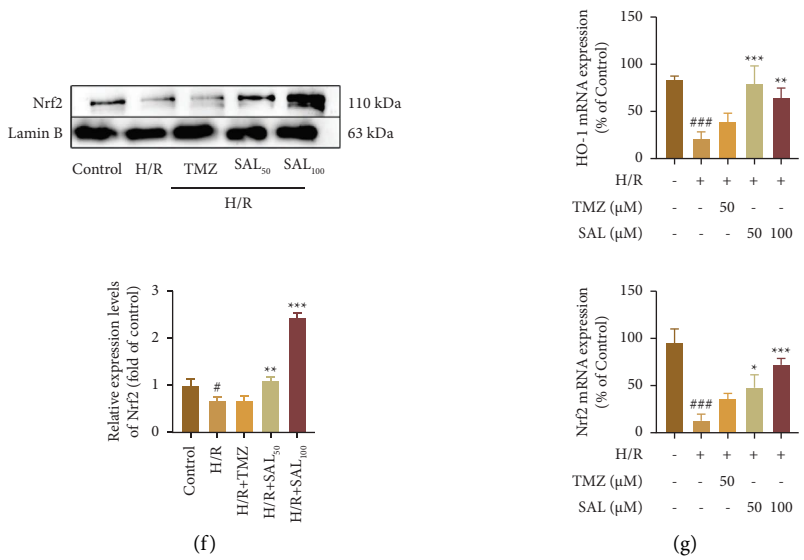

Figure 2: Effects of SAL on oxidative stress in H/R-treated H9c2 cells. (a) The intracellular ROS levels in H9c2 cells were measured by flow cytometry. (b–d) MDA, GSH, and SOD commercial kits were used to detect the activities of MDA, GSH, and SOD in H9c2 cells. (e, f) Western blotting and (g) RT-PCR were used to measure the levels of Nrf2 and HO-1 after H/R injury. Values are presented as mean ± SEM. $^{###}P < 0.001$ versus the control group; $^{*}P < 0.05$, $^{**}P < 0.01$, and $^{***}P < 0.001$ versus the H/R group.

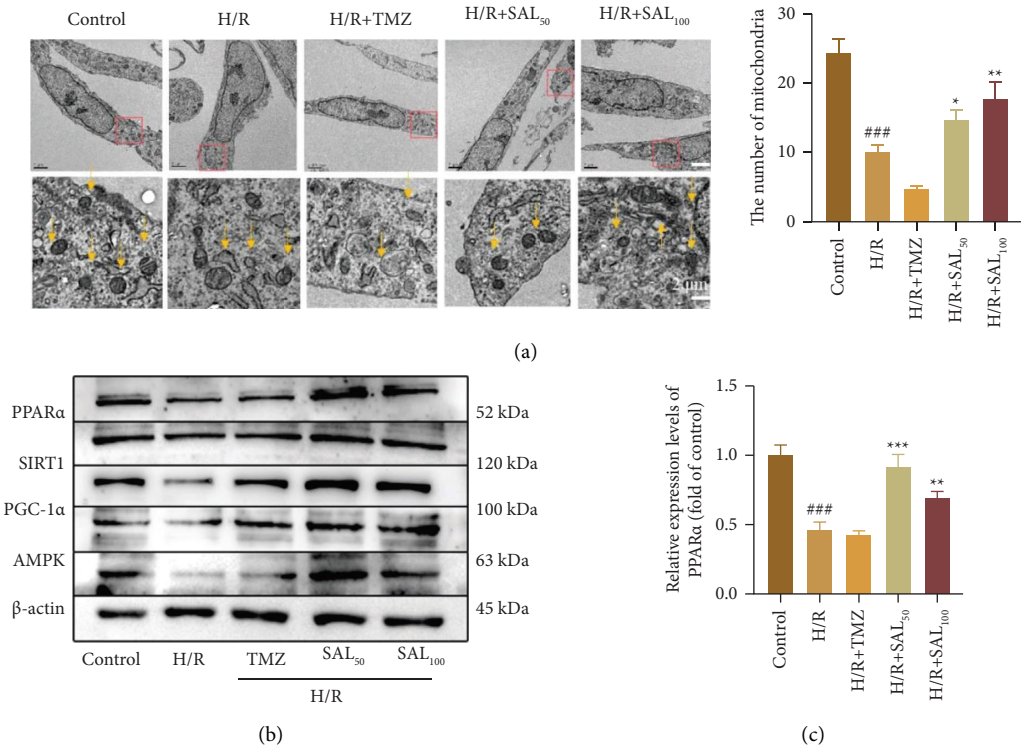

Figure 3: Continued.

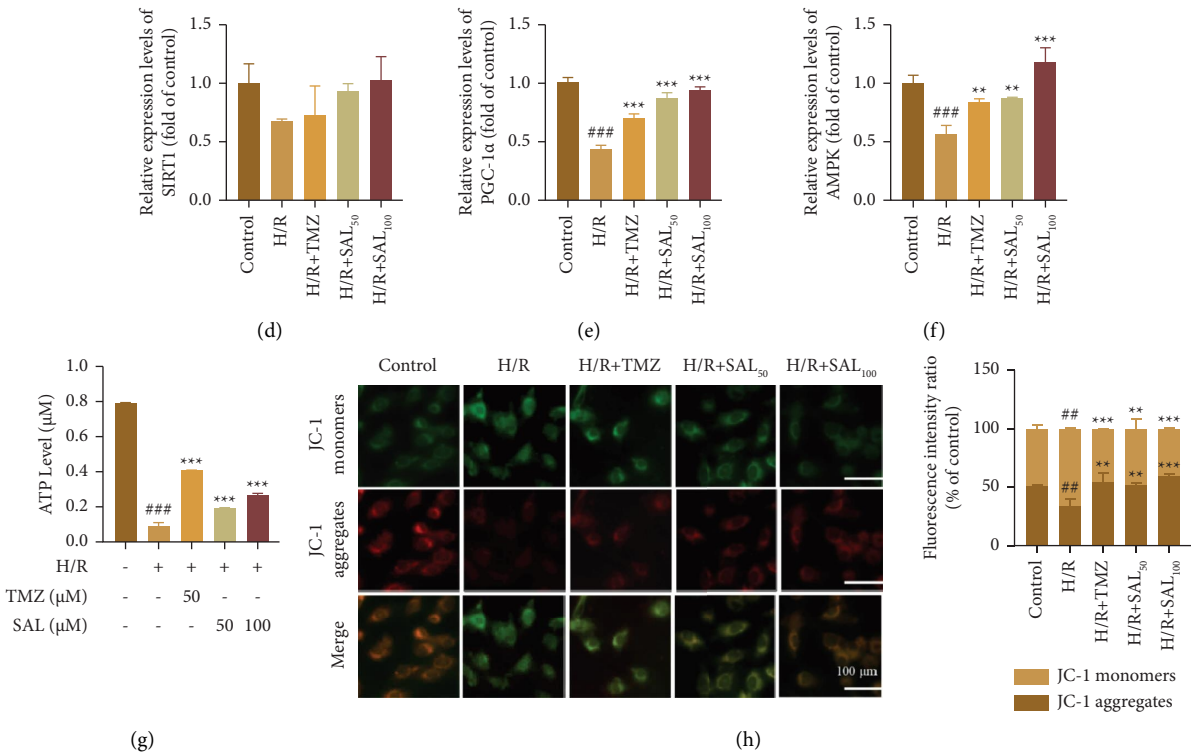

Figure 3: Effects of SAL on H/R-induced mitochondrial dysfunction of H9c2 cells. (a) TEM representative images of mitochondrial number; scale bar: 2 μm. (b–f) Western blotting was used to measure the levels of AMPK, SIRT1, PGC-1α, and PPARα after H/R injury. (g) ATP commercial kits were used to detect the activities of ATP in H9c2 cells. (h) Immunofluorescence staining of JC-1. Values are presented as mean ± SEM. $^{###}P < 0.001$ versus the control group; $^{**}P < 0.01$ and $^{***}P < 0.001$ versus the H/R group.

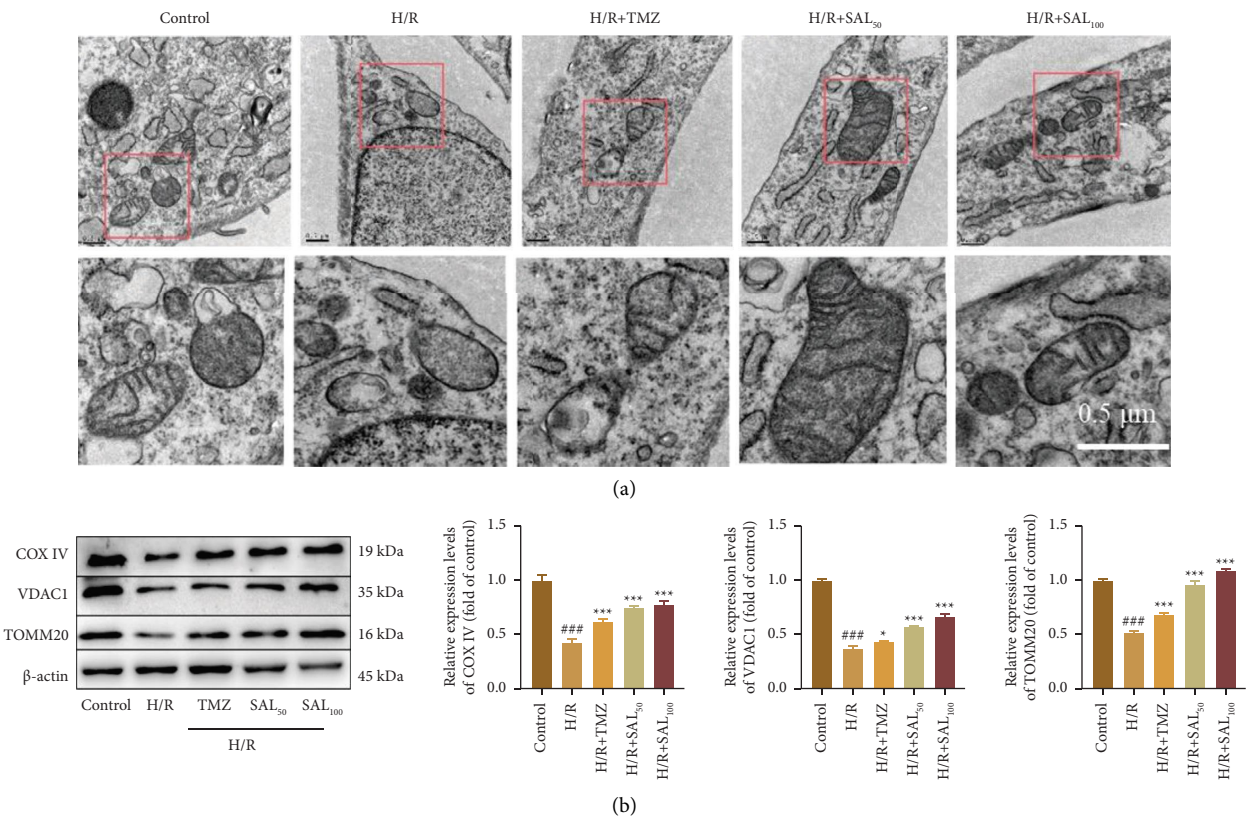

Figure 4: Continued.

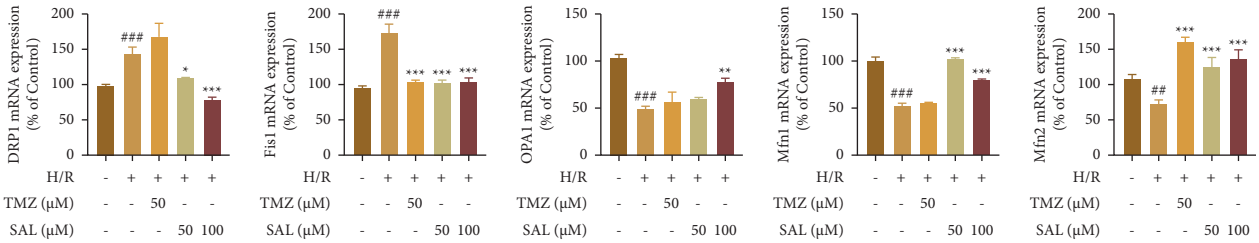

Figure 4: Effects of SAL on H/R-induced mitochondrial morphology of H9c2 cells. (a) TEM representative images of mitochondrial; scale bar: 0.5 μm. (b) Western blotting was used to measure the expression of VDAC1, COXIV, and TOMM20 after H/R injury. (c) PCR was used to analyze the transcription of Drp1, Fis1, OPA1, Mfn1, and Mfn2 after H/R injury. Values are presented as mean ± SEM. $^{###}P < 0.001$ versus the control group; $^{**}P < 0.01$ and $^{***}P < 0.001$ versus the H/R group.

vesicles as compared to the control group. Conversely, a substantial augmentation in autophagic vesicles was evident subsequent to the application of SAL therapy. This implies that SAL has the potential to induce autophagy since there was a significant boost in autophagic vesicles following its administration (Figure 5(a)). The western blotting analysis demonstrated that Beclin-1, LC3b, ATG5, and LAMP2 were repressed by HR injury. Interestingly, SAL upregulated the levels of these proteins in H9c2 cells (Figure 5(b)). Furthermore, during the occurrence of cardiac H/R injury, the expression of proteins associated with mitophagy was notably inhibited. However, SAL effectively mitigated the decline in PINK1 and Parkin levels across all experimental groups (Figure 5(c)). Furthermore, the translocation of Parkin was assessed by determining the expression of mito-Parkin and PINK1 (Figure 5(d)). During our study, we observed a significant decrease in the levels of mito-Parkin and PINK1 in the group subjected to H/R. Conversely, all samples treated with SAL exhibited an increase in the expression of mito-Parkin and PINK1, when compared to the H/R group. Furthermore, the expressions of cyto-Parkin and PINK1 were observed to be markedly reduced in comparison to the control group. This suggests that cardiac H/R injury negatively impacted the process of mitophagy by downregulating the expression of Parkin. Collectively, our findings highlight the beneficial effects of SAL in enhancing autophagic and mitophagy processes in the context of cardiac H/R injury.

3.6. SAL Mitigated H/R-Induced Damage in H9c2 Cells via Nrf2. Molecular docking was performed between SAL and Nrf2 (Figure 6(a)). The docking results showed that the binding energy of SAL to Nrf2 was −7.19 kcal-mol^{-1}, indicating good binding ability between the small molecule and the ligand. Five residues of SAL bound to Nrf2, namely, VAL-606, VAL-415, VAL-418, ARG-415, and GLY-367. The amino acid residues of the protein and the ligand formed a total of 10 hydrogen bonds, with a high number of bound hydrogen bonds and a small average distance, indicating that SAL can match well with the active pocket of Nrf2. As shown in Figure 6(b), between 45°C and 62°C, Nrf2 was relatively stable in SAL-treated cells. The findings suggest that SAL indeed exhibits the capability to bind to the Nrf2 protein, thereby enhancing its thermal stability within cardiomyocytes.

To investigate the correlation between oxidative stress and mitochondria, the Nrf2 antagonist ML385 (5 μM) was employed in examining the protective role of Nrf2 in mitochondrial function within H9c2 cells. Our observations (Figure 6(c)) revealed that the presence of the Nrf2 inhibitor ML385 impeded the protective influence of SAL on the survival of H9c2 cells. We subsequently assessed the levels of AST and LDH induced by ML385. The findings revealed a notable suppression of SAL's safeguarding influence on myocardial injury (Figures 6(d)–6(e)).

3.7. SAL Protected Mitochondrial Function against H/R-Induced Injury via Targeting Nrf2. Following that, our study focused on the examination of mitochondrial marker proteins, including VDAC1, COXIV, and TOMM20, subsequent to the administration of ML385. Our findings exhibited a reversal of augmented expression of mitochondrial compartmental proteins due to SAL following ML385 treatment (Figure 7(a)). Based on the qRT-PCR findings, it was observed that the administration of ML385 led to a substantial reversion in SAL-related protein expression associated with mitochondrial dynamics (as depicted in Figure 7(b)). By utilizing western blotting analysis, it was further evidenced that ML385 exhibited a significant reversal in the expression of crucial mitochondrial functional proteins, namely, PPARα, PGC-1α, and AMPK, concurrent with the presence of SAL (Figure 7(c)). The findings proposed that the blocking agent of Nrf2 and ML385 reversed the safeguarding impact of SAL on mitochondrial dysfunction caused by H/R.

3.8. SAL Promoted Autophagy and Mitophagy against H/R-Induced Injury via Targeting Nrf2. The expression of autophagy-related proteins LC3b, ATG5, LAMP2, and Beclin1 was effectively reversed by ML385 according to the western blotting results, which demonstrated the significant impact of ML385 on countering the increase induced by SAL (Figure 8(a)). Activation of mitophagy-related protein Parkin and PINK1 expression and mRNA levels by SAL were also significantly inhibited

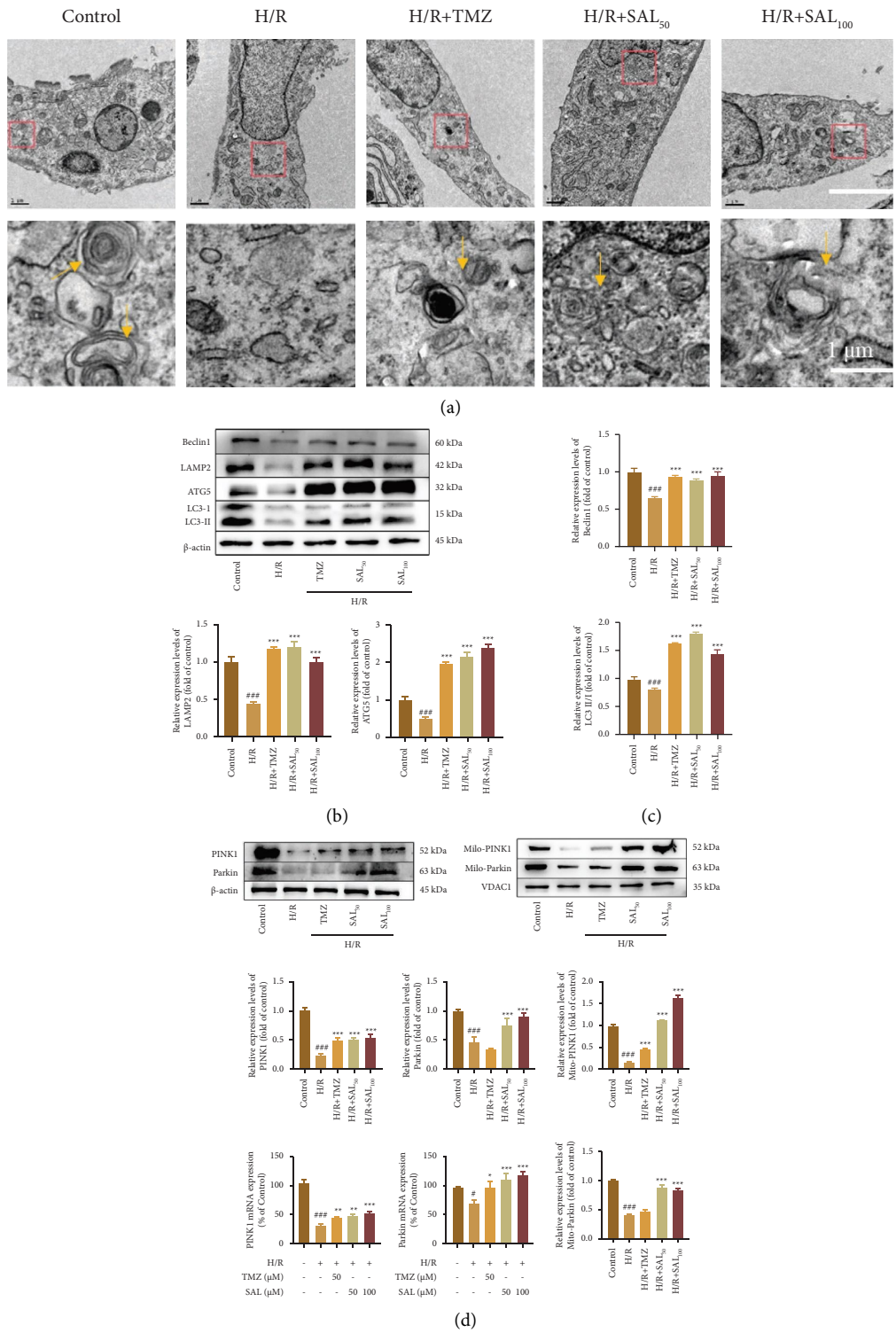

Figure 5: SAL improved autophagy and mitophagy under H/R injury. (a) TEM representative images of autophagosome; scale bar: 1 μm. (b–d) Western blotting and PCR were used to measure the levels of Beclin-1, LC3b, ATG5, LAMP2, Parkin, and PINK1 after H/R injury. Values are presented as mean ± SEM. $^{###}P < 0.001$ versus the control group; $^{***}P < 0.001$ versus the H/R group.

(Figure 8(b)). The findings from the analysis revealed that ML385 effectively counteracted the activation of autophagy and mitophagy caused by SAL, consequently nullifying the defensive properties of SAL in safeguarding against myocardial damage induced by H/R.

4. Discussion

The specific mechanism of action for the effect of maintaining mitochondrial homeostasis on H/R-exposed cardiomyocytes remains unclear [27]. In this particular investigation, we

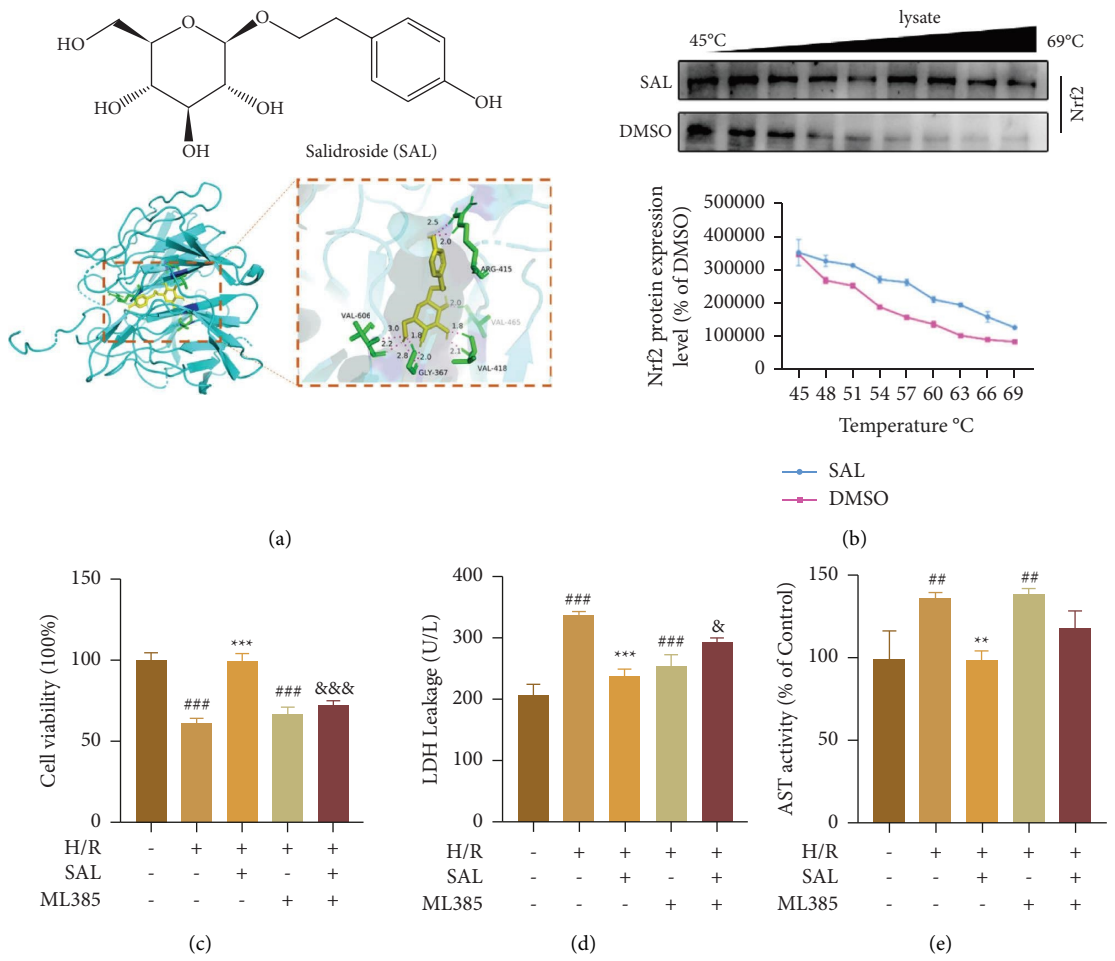

Figure 6: SAL ameliorated H/R-induced injury in H9c2 cells via Nrf2. (a) Molecular docking between SAL and Nrf2. (b) Cellular thermal shift assay (CETSA) was used to determine the effect of SAL on Nrf2 protein stability. (c) Cell viability of H9c2 cells treated with ML385 (5 μM). (d, e) The AST and LDH release of H9c2 cells treated with ML385 (5 μM) followed by H/R stimulation.

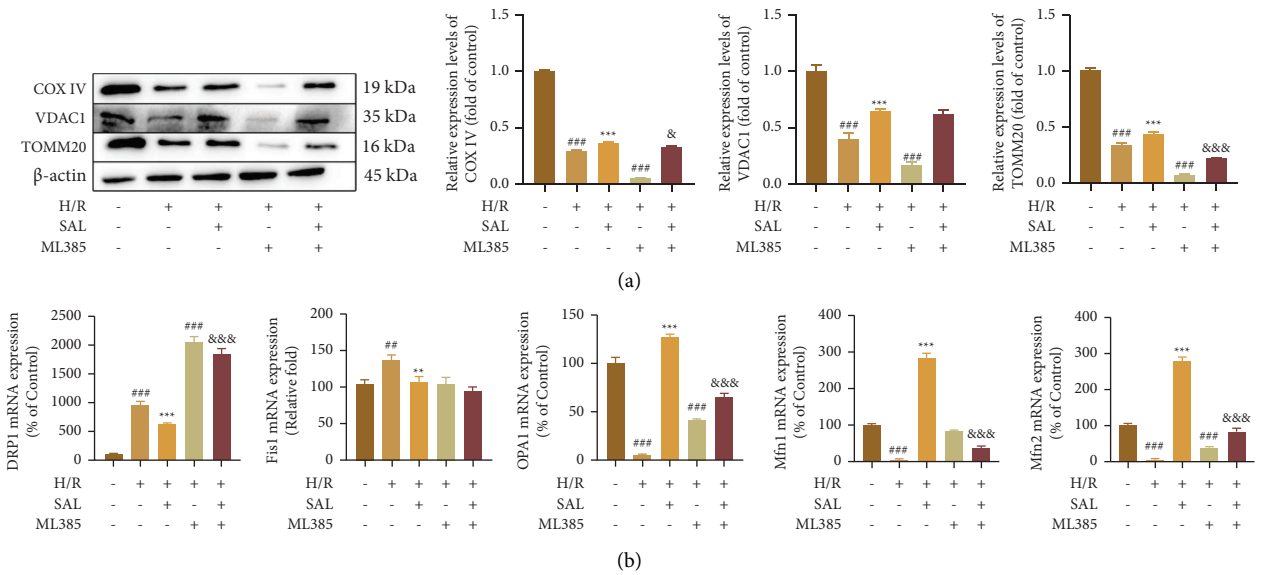

Figure 7: Continued.

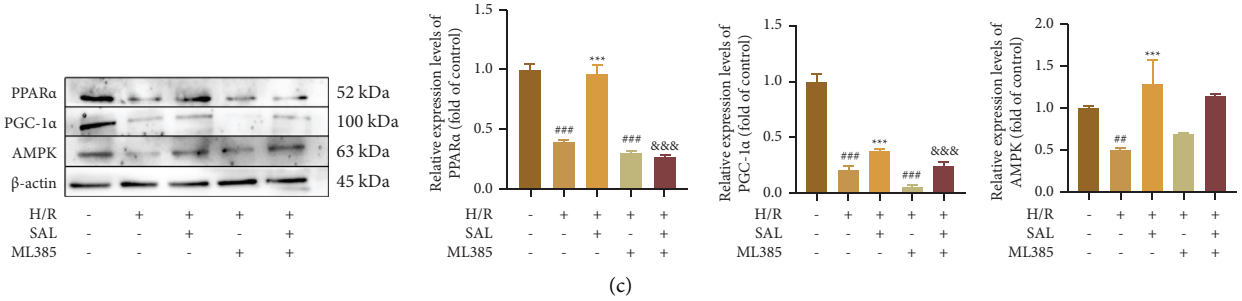

Figure 7: Inhibition of Nrf2 prevents the protective effect of SAL on mitochondrial function against H/R injury in H9c2. (a) Western blotting was used to measure the expression of COX IV, VDAC1, and TOMM20 after H/R injury. (b) PCR was used to analyze the transcription of Drp1, Fis1, OPA1, Mfn1, and Mfn2 after H/R injury. (c) Western blotting was used to measure the expression of AMPK, PGC-1α, and PPARα after H/R injury. Values are presented as mean ± SEM. $^{\#}P < 0.05$, $^{\#\#}P < 0.01$, and $^{\#\#\#}P < 0.001$ versus the control group; $^{**}P < 0.01$ and $^{***}P < 0.001$ versus the H/R group; $^{\&}P < 0.05$, $^{\&\&}P < 0.01$, and $^{\&\&\&}P < 0.001$ versus the SAL group; $^{\$}P < 0.05$, $^{\$\$}P < 0.01$, and $^{\$\$}P < 0.001$ versus the ML group.

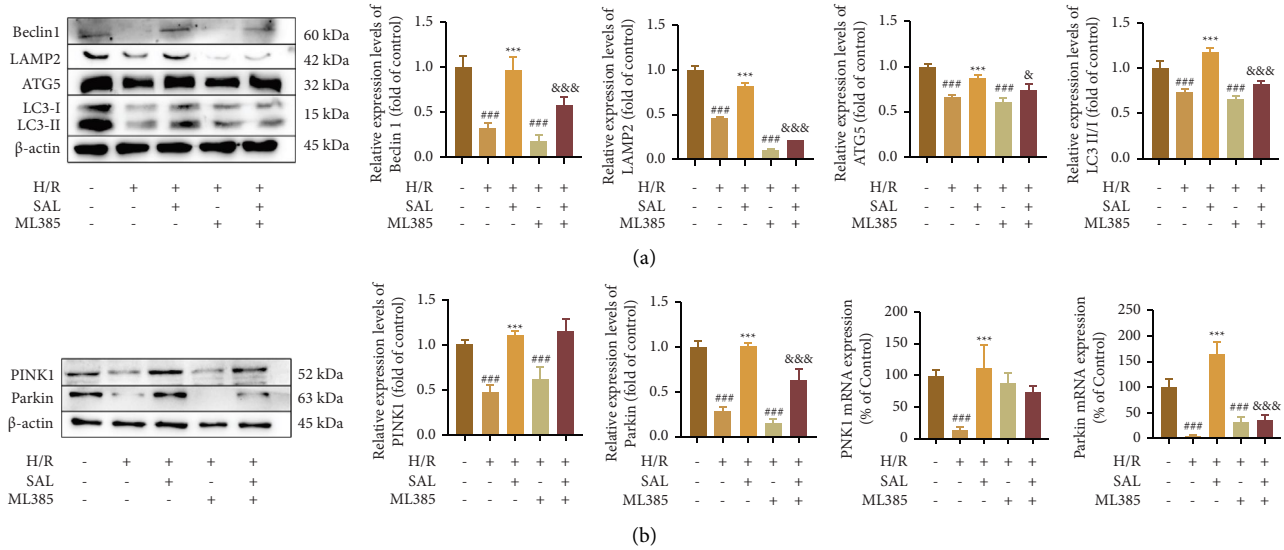

Figure 8: (a) Western blot was used to measure the expressions of Beclin-1, LC3b, ATG5, and LAMP2. (b) Western blot and PCR were used to measure the levels of Parkin and PINK1 after H/R injury. Values are presented as mean ± SE. $^{\#\#\#}P < 0.001$ versus the control group; $^{***}P < 0.001$ versus the H/R group; $^{\&}P < 0.05$, $^{\&\&}P < 0.01$, and $^{\&\&\&}P < 0.001$ versus the SAL group; $^{\$}P < 0.05$, $^{\$\$}P < 0.01$, and $^{\$\$}P < 0.001$ versus the ML group.

furnish substantiation to elucidate the safeguarding influence of SAL against the injury in H9c2 cells caused by H/R, accomplished by enhancing the function of the mitochondria. Our exploration discovered that SAL has the capability to alleviate oxidative stress caused by H/R in cardiomyocytes of H9c2 through the Nrf2/HO-1 pathway and preserve the balance of mitochondria from both their structure and performance. SAL can activate mitophagy through the Parkin/PINK1 pathway and improve mitochondrial dynamic imbalance. Furthermore, the AMPK/PGC-1α/PPARα signaling pathway is enhanced by SAL, leading to an amelioration of mitochondrial dysfunction. Our findings support the notion that SAL effectively safeguards against myocardial ischemia-reperfusion injury by preserving mitochondrial equilibrium.

Mitochondria play a crucial role in eukaryotic cells as vital organelles. By undergoing adaptive remodeling within living cells, these organelles ensure the maintenance of both their shape and function, achieving a state of consistent equilibrium referred to as mitochondrial homeostasis [28, 29]. In the occurrence of myocardial ischemia reperfusion, extensive generation of ROS induces oxidative stress, leading to mitochondrial impairment [30]. Our study found that in H/R-induced H9c2, ROS levels were significantly increased and oxidative stress indicators MDA, GSH, and SOD levels were significantly decreased, which was significantly reversed by SAL treatment. Nrf2 responds to oxidative stress by enhancing the expression of antioxidant and detoxifying enzymes, thereby countering the harmful effects of ROS and toxic metabolites [31]. HO-1 is a typical downstream gene of Nrf2 and is often used as a biomarker of Nrf2 activation [32]. The levels of HO-1 and Nrf2 in H9c2 cells were observed to be considerably enhanced by SAL according to our research on H/R-induced deterioration. In addition, the augment of Nrf2 and HO-1 expressions was

apparent upon administration of a high dose of SAL. Our findings fully demonstrate that it has a good ability to resist oxidative stress. When oxidative stress alters mitochondrial health, mitochondrial dysfunction occurs [33]. Mitochondrial dysfunction means reduced mitochondrial respiration capacity, decreased mitochondrial membrane potential, and reduced ATP production [34]. PGC-1α, a pivotal controller of the generation of mitochondria [35], can combine with various transcription factors such as PPARα, SIRT1, and AMPK to improve mitochondrial oxidative phosphorylation and fatty acid oxidation capacity, promote mitochondrial biosynthesis, and protect mitochondrial function [36]. Our study revealed an intriguing discovery: within the H/R group, the protein levels of PGC-1α, PPARα, and AMPK experienced a substantial reduction. However, upon administering varying doses of SAL treatment, this circumstance underwent a remarkable reversal. SAL's ability to enhance mitochondrial function by activating the AMPK/PGC-1α/PPARα pathway was clearly shown by this evidence, showcasing its effectiveness in boosting ATP production and providing cardioprotective benefits. The impact of SIRT1 was not found to be statistically significant in this context.

When mitochondrial health is compromised, in addition to mitochondrial dysfunction, mitochondrial morphology changes [37]. Mitochondrial morphology is regulated by mitophagy and mitochondrial dynamics [38]. Mitochondria exhibit a unique characteristic of constantly transitioning between elongated interconnected networks and fragmented disconnected arrangements. This ability to alter their shape and structure is facilitated by the mechanisms of mitochondrial fusion and fission [39]. The regulation of mitochondrial dynamics is under the responsibility of proteins involved in mitochondrial fusion (Mfn1, Mfn2, and OPA1) and proteins involved in mitochondrial fission (DRP1 and Fis1) [40]. Cardioprotective effects have been observed in the case of H/R when inhibiting the fission of mitochondria and promoting their fusion. Remarkably, our investigation revealed that the expressions of DRP1 and Fis1, which are involved in mitochondrial fission, along with the expressions of OPA1, Mfn1, and Mfn2, proteins related to mitochondrial fusion, underwent a noticeable reduction during H/R conditions. Interestingly, diverse quantities of SAL were administered throughout the experiment. After treatment, this condition was significantly improved. On the other hand, mitochondrial morphology is regulated by mitophagy [41]. Autophagy plays a crucial role in alleviating nutrient deficiencies by recycling intracellular components. In addition, it functions to maintain quality control by selectively eliminating organelles and regulating their numbers [42]. Our results showed that SAL could activate the expression of autophagy-related proteins LC3b, ATG5, LAMP2, and Beclin1, thereby inducing autophagy. Furthermore, mitophagy, which denotes the selective removal of mitochondria through the autophagic process, was also identified [43]. The regulation of selective autophagy of impaired mitochondria is possible in numerous cell types thanks to the Parkin and PINK1 genes [44]. Our results show that SAL can promote the expression of Parkin and PINK1 proteins and activate mitophagy to protect against myocardial injury. The complete results clearly illustrate that SAL effectively eliminates mitochondria via autophagy. In addition, it regulates alterations in the steady-state number of mitochondria needed to fulfill metabolic requirements while simultaneously promoting mitochondrial biogenesis. Moreover, the SAL treatment in the high-dose group exhibits enhanced myocardial injury protection. Subsequently, to investigate the mechanism of action in depth, we added the key protein Nrf2 inhibitor ML385 to detect mitochondria-associated proteins. According to the findings, ML385 inclusion negated the beneficial impact of SAL on the mitochondrial dysfunction mediated by AMPK/PGC-1α/PPARα. In addition, it disrupted the safeguarding effects of SAL-induced autophagy in mitigating mitochondrial impairment, while partially hindering the activation of Parkin and PINK1 proteins.

Our research thoroughly exhibited that SAL effectively demonstrated cardioprotective properties amidst H/R and unveiled that the safeguarding impact on the myocardial injury caused by H/R was accomplished through the preservation of mitochondrial equilibrium. This study showed meticulously and comprehensively the mechanism of SAL's cardioprotective effects and provided some new ideas for the treatment of I/R. It also provides some basis for the development of Rhodiola Rosea glycosides as a cardioprotective functional food compound.

Data Availability

The data used to support the findings of this study are available from the corresponding author upon request.

Conflicts of Interest

The authors declare that there are no conflicts of interest.

Authors' Contributions

Tingxu Yan and Xu Li contributed equally to this work.

Acknowledgments

This research was supported by Special Funds for Transformation and Upgrading of Industrial Informatization of Industry and Information Technology Department of Jiangsu (2020): Key Technologies of Multi-Component Traditional Chinese Medicines and the National Natural Science Foundation of China (No. 82173961).

References

[1] F. Wu, W. Huang, Q. Tan et al., "ZFP36L2 regulates myocardial ischemia/reperfusion injury and attenuates mitochondrial fusion and fission by LncRNA PVT1," *Cell Death & Disease*, vol. 12, no. 6, p. 614, 2021.

[2] Q. M. Chen, "Nrf2 for cardiac protection: pharmacological options against oxidative stress," *Trends in Pharmacological Sciences*, vol. 42, no. 9, pp. 729–744, 2021.

[3] J. Han, Q. Li, Z. Ma, and J. Fan, "Effects and mechanisms of compound Chinese medicine and major ingredients on microcirculatory dysfunction and organ injury induced by

ischemia/reperfusion," *Pharmacology & Therapeutics*, vol. 177, pp. 146–173, 2017.

[4] M. Song, A. Franco, J. Fleischer, L. Zhang, and G. Dorn, "Abrogating mitochondrial dynamics in mouse hearts accelerates mitochondrial senescence," *Cell Metabolism*, vol. 26, no. 6, pp. 872–883.e5, 2017.

[5] V. Varshney, A. Kumar, V. Parashar, A. Kumar, A. Goyal, and D. Garabadu, "Therapeutic potential of capsaicin in various neurodegenerative diseases with special focus on Nrf2 signaling," *Current Pharmaceutical Biotechnology*, vol. 25, 2024.

[6] R. Zou, W. Shi, J. Qiu et al., "Empagliflozin attenuates cardiac microvascular ischemia/reperfusion injury through improving mitochondrial homeostasis," *Cardiovascular Diabetology*, vol. 21, no. 1, p. 106, 2022.

[7] H. Zhou, S. Hu, Q. Jin et al., "Mff-Dependent mitochondrial fission contributes to the pathogenesis of cardiac microvasculature ischemia/reperfusion injury via induction of mROS-mediated cardiolipin oxidation and HK2/VDAC1 disassociation-involved mPTP opening," *Journal of the American Heart Association*, vol. 6, no. 3, 2017.

[8] N. N. Wu, Y. Zhang, and J. Ren, "Mitophagy, mitochondrial dynamics, and homeostasis in cardiovascular aging," *Oxidative Medicine and Cellular Longevity*, vol. 2019, Article ID 9825061, 15 pages, 2019.

[9] C. Maneechote, S. Palee, S. Kerdphoo, T. Jaiwongkam, S. Chattipakorn, and N. Chattipakorn, "Balancing mitochondrial dynamics via increasing mitochondrial fusion attenuates infarct size and left ventricular dysfunction in rats with cardiac ischemia/reperfusion injury," *Clinical Science*, vol. 133, no. 3, pp. 497–513, 2019.

[10] J. Hao, J. Zhou, S. Hu et al., "RTA 408 ameliorates diabetic cardiomyopathy by activating Nrf2 to regulate mitochondrial fission and fusion and inhibiting NF-κB-mediated inflammation," *American Journal of Physiology- Cell Physiology*, vol. 326, no. 2, pp. C331–C347, 2024.

[11] J. Zhang, W. Lv, G. Zhang et al., "Nrf2 and mitochondria form a mutually regulating circuit in the prevention and treatment of metabolic syndrome," *Antioxidants and Redox Signaling*, vol. 23, 2024.

[12] J. Zhou, J. Hao, Z. Zhong et al., "Fecal microbiota transplantation in mice exerts a protective effect against doxorubicin-induced cardiac toxicity by regulating nrf2-mediated cardiac mitochondrial fission and fusion," *Antioxidants and Redox Signaling*, vol. 30, 2023.

[13] C. Zhuo, J. Xin, W. Huang et al., "Irisin protects against doxorubicin-induced cardiotoxicity by improving AMPK-Nrf2 dependent mitochondrial fusion and strengthening endogenous anti-oxidant defense mechanisms," *Toxicology*, vol. 494, Article ID 153597, 2023.

[14] B. Ren, T. Zhang, Q. Guo et al., "Nrf2 deficiency attenuates testosterone efficiency in ameliorating mitochondrial function of the substantia nigra in aged male mice," *Oxidative Medicine and Cellular Longevity*, vol. 2022, Article ID 3644318, 33 pages, 2022.

[15] X. Niu, S. Pu, C. Ling et al., "lncRNA Oip5-as1 attenuates myocardial ischaemia/reperfusion injury by sponging miR-29a to activate the SIRT1/AMPK/PGC1α pathway," *Cell Proliferation*, vol. 53, no. 6, Article ID e12818, 2020.

[16] M. Lampert, A. Orogo, R. Najor et al., "BNIP3L/NIX and FUNDC1-mediated mitophagy is required for mitochondrial network remodeling during cardiac progenitor cell differentiation," *Autophagy*, vol. 15, no. 7, pp. 1182–1198, 2019.

[17] J. Qiang, R. Yang, X. Li et al., "Monotropein induces autophagy through activation of the NRF2/PINK axis, thereby alleviating sepsis-induced colonic injury," *International Immunopharmacology*, vol. 127, Article ID 111432, 2024.

[18] E. Zhang, T. Wu, Y. Zhuo et al., "Effect of Nrf2 on brain injury induced by hydraulic shock via regulation of mitophagy and apoptosis," *Aging*, vol. 15, no. 22, pp. 13422–13433, 2023.

[19] X. Chao, S. Wang, S. Fulte et al., "Hepatocytic p62 suppresses ductular reaction and tumorigenesis in mouse livers with mTORC1 activation and defective autophagy," *Journal of Hepatology*, vol. 76, no. 3, pp. 639–651, 2022.

[20] B. Sun, Y. Xu, Z. Liu, W. Meng, and H. Yang, "Autophagy assuages myocardial infarction through Nrf2 signaling activation-mediated reactive oxygen species clear," *European Review for Medical and Pharmacological Sciences*, vol. 24, no. 13, pp. 7381–7390, 2020.

[21] L. Zhu, Q. Zhang, C. Hua, and X. Ci, "Melatonin alleviates particulate matter-induced liver fibrosis by inhibiting ROS-mediated mitophagy and inflammation via Nrf2 activation," *Ecotoxicology and Environmental Safety*, vol. 268, Article ID 115717, 2023.

[22] C. Tang, H. Han, M. Yan et al., "PINK1-PRKN/PARK2 pathway of mitophagy is activated to protect against renal ischemia-reperfusion injury," *Autophagy*, vol. 14, no. 5, pp. 880–897, 2018.

[23] E. Panieri, S. Pinho, G. Afonso, P. Oliveira, T. Cunha-Oliveira, and L. Saso, "NRF2 and mitochondrial function in cancer and cancer stem cells," *Cells*, vol. 11, no. 15, p. 2401, 2022.

[24] X. Zhang, L. Xie, J. Long et al., "Salidroside: a review of its recent advances in synthetic pathways and pharmacological properties," *Chemico-Biological Interactions*, vol. 339, Article ID 109268, 2021.

[25] T. Yan, X. Li, T. Nian et al., "Salidroside inhibits ischemia/reperfusion-induced myocardial apoptosis by targeting mir-378a-3p via the igf1r/pi3k/akt signaling pathway," *Transplantation Proceedings*, vol. 54, no. 7, pp. 1970–1983, 2022.

[26] Y. Zhang, Y. Wang, J. Xu et al., "Melatonin attenuates myocardial ischemia-reperfusion injury via improving mitochondrial fusion/mitophagy and activating the AMPK-OPA1 signaling pathways," *Journal of Pineal Research*, vol. 66, no. 2, Article ID e12542, 2019.

[27] H. Zhou, P. Zhu, J. Wang, H. Zhu, J. Ren, and Y. Chen, "Pathogenesis of cardiac ischemia reperfusion injury is associated with CK2α-disturbed mitochondrial homeostasis via suppression of FUNDC1-related mitophagy," *Cell Death & Differentiation*, vol. 25, no. 6, pp. 1080–1093, 2018.

[28] A. Mohanty, R. Tiwari-Pandey, and N. R. Pandey, "Mitochondria: the indispensable players in innate immunity and guardians of the inflammatory response," *J Cell Commun Signal*, vol. 13, no. 3, pp. 303–318, 2019.

[29] L. Xie, F. Shi, Z. Tan, Y. Li, A. Bode, and Y. Cao, "Mitochondrial network structure homeostasis and cell death," *Cancer Science*, vol. 109, no. 12, pp. 3686–3694, 2018.

[30] B. Y. Nguyen, A. Ruiz-Velasco, T. Bui, L. Collins, X. Wang, and W. Liu, "Mitochondrial function in the heart: the insight into mechanisms and therapeutic potentials," *British Journal of Pharmacology*, vol. 176, no. 22, pp. 4302–4318, 2019.

[31] T. Wang, T. Zhou, M. Xu et al., "Platelet membrane-camouflaged nanoparticles carry microRNA inhibitor against myocardial ischaemia–reperfusion injury," *Journal of Nanobiotechnology*, vol. 20, no. 1, p. 434, 2022.

[32] H. Ji, F. Xiao, S. Li, R. Wei, F. Yu, and J. Xu, "GRP78 effectively protect hypoxia/reperfusion-induced myocardial apoptosis via promotion of the Nrf2/HO-1 signaling pathway," *Journal of Cellular Physiology*, vol. 236, no. 2, pp. 1228–1236, 2021.

[33] H. Yang, W. Xue, C. Ding et al., "Vitexin mitigates myocardial ischemia/reperfusion injury in rats by regulating mitochondrial dysfunction via epac1-rap1 signaling," *Oxidative Medicine and Cellular Longevity*, vol. 2021, Article ID 9921982, 17 pages, 2021.

[34] E. Bulthuis, M. Adjobo-Hermans, P. Willems, and W. Koopman, "Mitochondrial morphofunction in mammalian cells," *Antioxidants and Redox Signaling*, vol. 30, no. 18, pp. 2066–2109, 2019.

[35] J. Shin, H. Ko, H. Kang et al., "PARIS (ZNF746) repression of PGC-1α contributes to neurodegeneration in Parkinson's disease," *Cell*, vol. 144, no. 5, pp. 689–702, 2011.

[36] L. Chen, Y. Qin, B. Liu et al., "PGC-1α-Mediated mitochondrial quality control: molecular mechanisms and implications for heart failure," *Frontiers in Cell and Developmental Biology*, vol. 10, Article ID 871357, 2022.

[37] F. R. Jornayvaz and G. I. Shulman, "Regulation of mitochondrial biogenesis," *Essays in Biochemistry*, vol. 47, pp. 69–84, 2010.

[38] J. Hu, L. Zhang, F. Fu et al., "Cardioprotective effect of ginsenoside Rb1 via regulating metabolomics profiling and AMP-activated protein kinase-dependent mitophagy," *Journal of Ginseng Research*, vol. 46, no. 2, pp. 255–265, 2022.

[39] J. Gollmer, A. Zirlik, and H. Bugger, "Mitochondrial mechanisms in diabetic cardiomyopathy," *Diabetes & Metabolism Journal*, vol. 44, no. 1, pp. 33–53, 2020.

[40] G. Twig, A. Elorza, A. Molina et al., "Fission and selective fusion govern mitochondrial segregation and elimination by autophagy," *The EMBO Journal*, vol. 27, no. 2, pp. 433–446, 2008.

[41] J. Ye, M. Wang, R. Wang et al., "Hydroxysafflor yellow A inhibits hypoxia/reoxygenation-induced cardiomyocyte injury via regulating the AMPK/NLRP3 inflammasome pathway," *International Immunopharmacology*, vol. 82, Article ID 106316, 2020.

[42] O. Yamaguchi, "Autophagy in the heart," *Circulation Journal*, vol. 83, no. 4, pp. 697–704, 2019.

[43] G. López-Doménech, C. Covill-Cooke, J. H. Howden et al., "Miro ubiquitination is critical for efficient damage-induced PINK1/Parkin-mediated mitophagy," *BioRxiv*, vol. 25, 2018.

[44] Y. Chun and J. Kim, "Autophagy: an essential degradation program for cellular homeostasis and life," *Cells*, vol. 7, no. 12, p. 278, 2018.